JSS Focus Issue on Gallium Oxide Based Materials and Devices

Eu Activation in β-Ga_2O_3 MOVPE Thin Films by Ion Implantation

M. Peres,[1] E. Nogales,[2] B. Mendez,[2] K. Lorenz,[1,3] M. R. Correia,[4] T. Monteiro,[4] and N. Ben Sedrine[4,z]

[1]*IPFN, Instituto Superior Técnico, Campus Tecnológico e Nuclear, P-2695-066 Bobadela LRS, Portugal*
[2]*Dpto. Física de Materiales, Universidad Complutense de Madrid, 28040 Madrid, Spain*
[3]*Instituto de Engenharia de Sistemas de Computadores - Microsistemas e Nanotecnologia (INESC-MN), Lisboa, Portugal*
[4]*Departamento de Física e I3N, Universidade de Aveiro, Campus Universitário de Santiago, 3810-193 Aveiro, Portugal*

In this work, we have established the effects of Eu implantation and annealing on β-Ga_2O_3 thin films grown by metal organic vapor phase epitaxy (MOVPE) on sapphire substrate. The study is based on the combined information from structural and optical techniques: X-ray diffraction (XRD), Rutherford backscattering spectrometry (RBS), cathodoluminescence (CL), photoluminescence (PL), and photoluminescence excitation (PLE). The thin films were implanted with a fluence of 1×10^{15} Eu·cm^{-2} and annealed at 900°C. Neither significant changes in peak width or position nor additional peaks related to Eu complexes were detected in the XRD 2θ-ω scans. RBS results and SRIM simulation are in good agreement, revealing that no Eu diffusion to the surface occurs during annealing. For the used implantation/annealing conditions, the Eu ion penetration depth reached ∼130 nm, with a maximum concentration at ∼50 nm. Furthermore, CL and PL/PLE results evidenced the optical activation of the Eu^{3+} in the β-Ga_2O_3 host. The detailed study of the Eu^{3+} intra-4*f* shell transitions revealed that at least one active site is created by the Eu implantation/annealing in β-Ga_2O_3 thin films grown on sapphire. Independently of the β-Ga_2O_3 film thickness, well controlled optical activation of implanted Eu was achieved.

 [DOI: 10.1149/2.0191907jss]

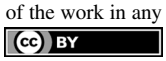

Manuscript received February 11, 2019. Published March 6, 2019. *This paper is part of the JSS Focus Issue on Gallium Oxide Based Materials and Devices.*

Monoclinic β-Ga_2O_3 has received increasing attention in the last few years thanks to its unique properties and its availability as a bulk substrate.[1–3] It is the transparent metal oxide material with the widest bandgap of ∼ 4.9 eV among the most practical ones. In comparison to Si, SiC and GaN materials,[4–7] the significantly higher breakdown field (8 MV/cm)[1,8] achieved for β-Ga_2O_3 makes it more suitable for high-power electronics. The transparency in the solar spectrum (especially in the ultra-violet (UV) region), the development of single crystal substrates, the good thermal/chemical stability, and the achievement of reasonable carrier mobility values, pave the way for the use of β-Ga_2O_3 in UV solar blind photodetectors, transparent field effect transistors, as well as UV harvesting solar cells, LEDs and lasers.[8–10] β-Ga_2O_3 is explored as a material for thin film electroluminescent devices, for which it is considered to be a good host for the optical activation of transition metals and rare earth (RE) ions,[11,12] similarly to nitride materials.[13–20] Electroluminescent devices with red emission and relatively low threshold voltages of (60 V) were achieved by adding a Ga_2O_3:Eu phosphor layer deposited by pulsed laser deposition on oxides.[21] Although restricted by the solubility limit of the RE in the β phase of Ga_2O_3, several studies were performed by in-situ Eu incorporation in β-Ga_2O_3 fibers,[22] nanocrystals,[23] and thin films.[12,24,25] RE implantation is used as an alternative process to overcome the solubility issue, and was successfully achieved for Eu-doped β-Ga_2O_3 nanowires and bulk single crystal.[26,27] In this work, we explore the Eu implantation and annealing in β-Ga_2O_3 thin films for their application in efficient red thin film luminescent devices.

Experimental

Three epitaxial thin films of β-Ga_2O_3, with the thicknesses of 118 nm (S1), 125 nm (S2) and 145 nm (S3), were deposited on (0001) sapphire substrate by metal organic vapor phase epitaxy (MOVPE). The thickness values were evaluated by spectroscopic ellipsometry and independently confirmed by scanning electron microscope (SEM) measurements. The sapphire substrates underwent thermal treatment in oxygen atmosphere at 950°C for 1 h before growth to obtain a damage-free surface with atomic steps. More details about the growth can be found in Ref. 28.

Ion implantation was carried out considering the optimized conditions for single crystals,[27] using 300 keV Eu ions at 600°C, with the fluence of 1×10^{15} Eu·cm^{-2}. Post-implant rapid thermal annealing was performed at the temperature of 900°C in flowing argon during 30 s in an ANNEALSYS rapid thermal processor. The Eu-profile simulation considering a material density of 5.95 g.cm^{-3},[29] was performed using the stopping and range of ions in matter (SRIM) Monte Carlo simulation code.[30] The structural characterization of the as-grown and Eu-implanted/annealed β-Ga_2O_3 thin films were performed by X-ray diffraction (XRD) using a Bruker D8 diffractometer. The primary beam is collimated using a Göbel mirror and a 0.6 mm slit. The diffracted X-rays were detected by a scintillation detector located behind long Soller slits.

The structure and composition of the samples were also analyzed by Rutherford backscattering spectrometry (RBS), with a 2 MeV α particle beam of 1 mm diameter obtained from a Van de Graaff accelerator. The random spectra were obtained by tilting the sample by 5 degrees and rotating the sample during the measurement. The backscattered particles were detected using two PIN diode detectors mounted at backscattering angles of 165° and 140°. The compositions, the Eu profile and the thicknesses were extracted as a function of depth by the fitting procedure using the nuclear data furnace code (NDF).[31–33]

Cathodoluminescence (CL) studies were performed at room temperature (RT) with a Hitachi S2500 scanning electron microscope (SEM) using an acceleration voltage of 3 kV, which corresponds to a penetration depth between 25 and 50 nm.[34] The CL spectra were recorded using a charge coupling device camera, Hamamatsu PMA–11.

Photoluminescence (PL) and PL excitation (PLE) spectra were recorded at RT using a Fluorolog-3 Horiba Scientific modular apparatus with a double additive grating scanning monochromator (2×180 mm, 1200 grooves·mm^{-1}) in the excitation channel and a triple grating iHR550 spectrometer (550 mm, 1200 grooves·mm^{-1}) coupled to a R928 Hamamatsu photomultiplier for detection. A 450 W Xe lamp was used as excitation source. The measurements were carried out,

[z]E-mail: bsnebiha@yahoo.fr; nbensedrine@ua.pt

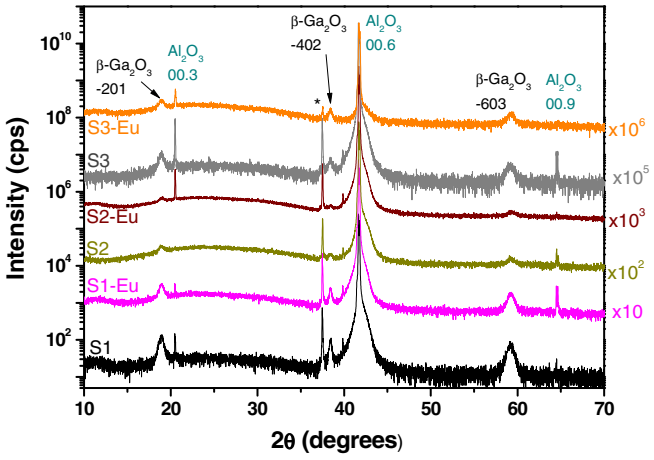

Figure 1. 2θ-ω scans of the as-grown epitaxial β-Ga_2O_3 thin films on sapphire with different thicknesses (the scans are multiplied by the factor on the right for clarity).

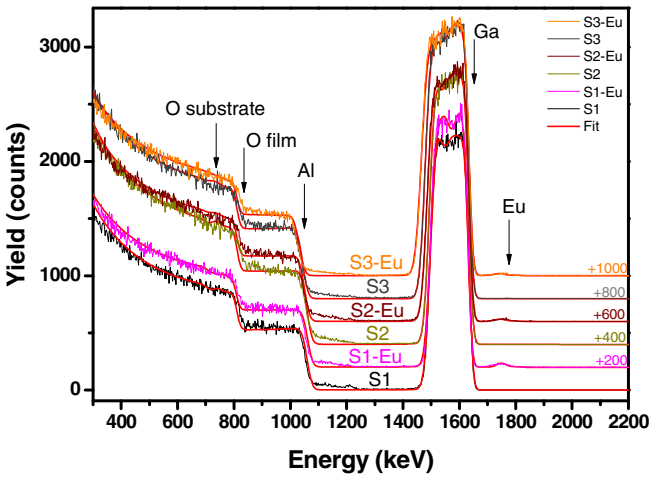

Figure 2. RBS spectra for the as-grown and Eu-implanted/annealed β-Ga_2O_3 thin films.

in the same experimental conditions, using the front face acquisition geometry, and corrected to the spectral response of the optical components and the Xe lamp. Further PL tests were realized using the vacuum ultraviolet (VUV) excitation on a Fluorimeter Horiba Scientific modular equipment with two monochromators (H20-UVL) (200 mm, 1200 grooves·mm^{-1}), one at the excitation and one at the emission. A D200VUV deuterium light source emitting from 115 to 370 nm was used as excitation source, with a maximum intensity at 160 nm.

Results and Discussion

In order to evaluate the structural quality of the films, 2θ-ω scans were performed and Fig. 1 depicts the XRD scans of the different β-Ga_2O_3 thin films on sapphire (S1, S2 and S3) and the Eu-implanted/annealed samples (S1-Eu, S2-Eu and S3-Eu). The sharp peaks at $2\theta = 21.0°$, 41.7° and 64.5° correspond to the 00.3, 00.6 and 00.9 Bragg reflections of the *c*-plane sapphire substrate, respectively. While the peaks at $2\theta = 18.9°$, 38.4°and 59.2° correspond to the β-Ga_2O_3 epitaxial layers, and are assigned to the −201, −402 and −603 Bragg reflections from the monoclinic β-Ga_2O_3 crystalline structure.[28,35–37] The peak at $2\theta = 37.5°$ (asterisk) is the K_β line corresponding to the 00.6 Bragg reflection. The presence of only one family of planes suggests that the as-grown β-Ga_2O_3 thin films are preferentially oriented with (−201) surface orientation and without additional phases. Furthermore, for the implanted and annealed β-Ga_2O_3 thin films (S1-Eu, S2-Eu and S3-Eu), neither additional peaks related to Eu complexes nor significant change of the peak width or position were detected.

Figure 2 shows the random RBS spectra of the as-grown and Eu-implanted/annealed β-Ga_2O_3 thin films with a fluence of 1×10^{15} Eu·cm^{-2}. These spectra are characterized by four barriers assigned to the Ga and O from the thin β-Ga_2O_3 film, then Al and O from the sapphire substrate. As expected, RBS spectra exhibit an increase of the barrier width assigned to Ga with increasing the β-Ga_2O_3 film thickness. In the implanted and annealed samples, the signal at high energy assigned to the implanted Eu is also detected. The spectra were fitted, using the NDF code considering a model of four layers plus substrate, in order to take into account the composition gradient with depth. The fits suggest that the films present a Ga/O ratio of ∼ 0.6, with a Ga content decreasing by 10% from the surface layer down to the layer right on top of the substrate. Furthermore, the fits also reveal that no significant stoichiometry changes occur after Eu-implantation and annealing. The comparison of the Eu profile measured by RBS with the SRIM simulation (Fig. 3), shows a fairly good agreement, revealing that no Eu diffusion to the surface occurs during annealing. For all samples and in the used implantation/annealing conditions, the Eu ion penetration depth reaches ∼130 nm, with a maximum concentration at ∼50 nm.

Fig. 4a represents RT CL spectra of the Eu-implanted/annealed β-Ga_2O_3 thin films (S1-Eu, S2-Eu and S3-Eu), compared with the ones obtained for β-Ga_2O_3 bulk single crystals.[27] The detailed implantation and annealing conditions are also indicated. The spectra present a broad UV band and sharp luminescence lines with dominant intensity. For clarity, Fig. 4b represents the UV-blue wavelength region. For the β-Ga_2O_3 thin films, the CL response exhibits a UV-band luminescence, typical for as-grown β-Ga_2O_3,[22,23,38–42] and commonly associated to intrinsic point defects, such as oxygen vacancies, gallium vacancies and oxygen-gallium vacancy pairs.[39,43–45] In addition to intrinsic defects, the UV band luminescence in β-Ga_2O_3 was reported to depend on doping[39,46] as well as implantation and annealing conditions.[26] For wavelengths above 520 nm in Fig. 4c, sharp luminescence lines are well resolved. These lines are characteristic of the Eu^{3+} intra-4*f* shell transitions, indicating that the used Eu implantation and annealing conditions efficiently incorporated the Eu^{3+} ions in the crystal lattice and optically activated the Eu^{3+} ions in β-Ga_2O_3 thin films. Furthermore, by comparing with PL response from Eu-implanted/annealed *c*-sapphire from Ref.47, we have confirmed that the observed transitions are not originating from Eu^{3+} ions incorporated in *c*-sapphire (not shown). It should be pointed out that besides the Eu^{3+} intra-4*f* shell transitions, typical Cr^{3+} emission corresponding to $^4T_2 \rightarrow {}^4A_2$

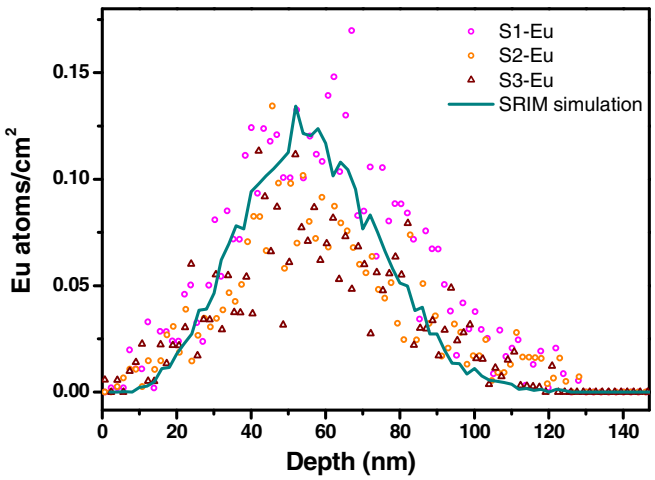

Figure 3. Eu profile measured by RBS compared with the one simulated by SRIM.

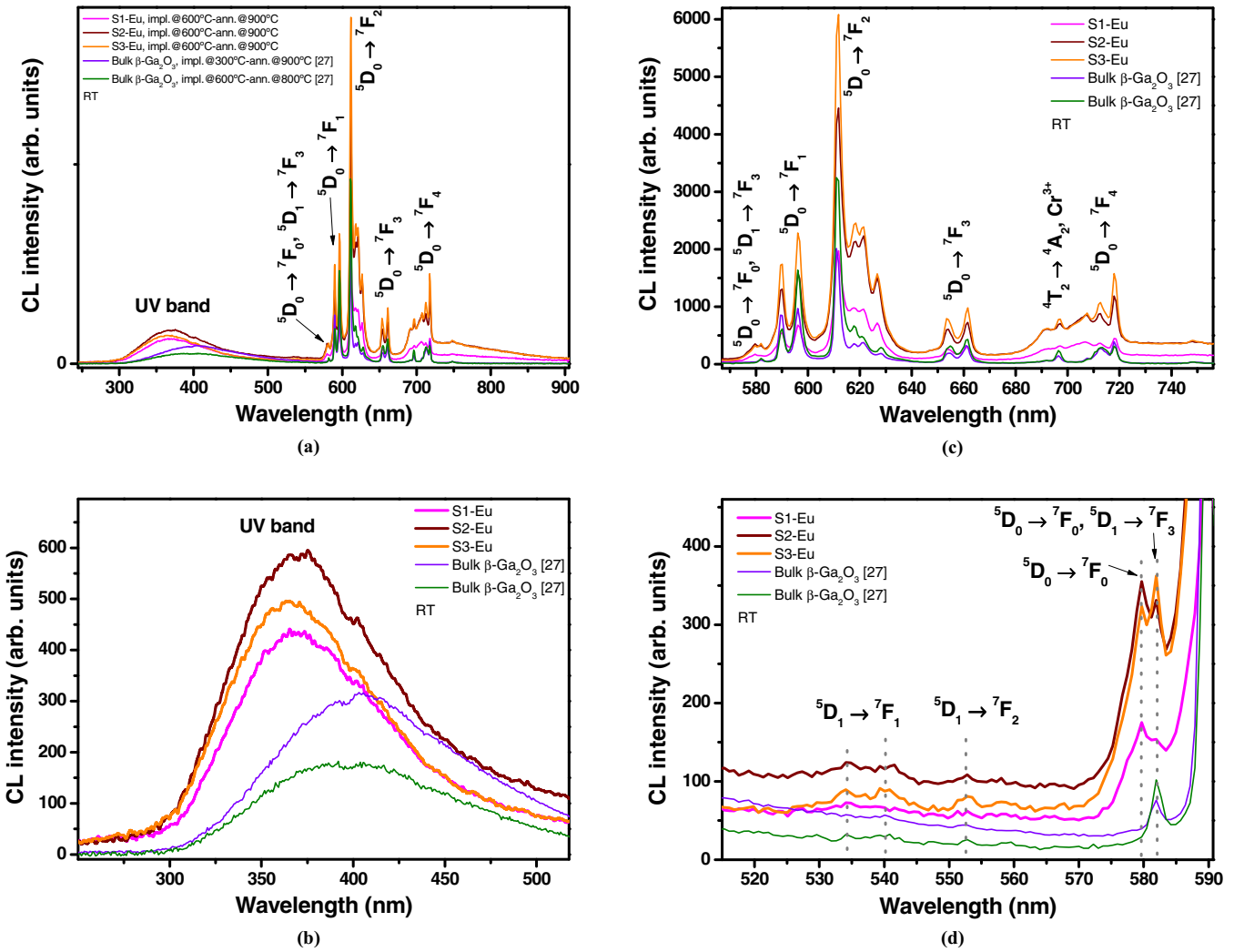

Figure 4. RT CL spectra of S1-Eu, S2-Eu and S3-Eu β-Ga_2O_3 thin films compared with Eu implanted/annealed bulk β-Ga_2O_3 samples at similar conditions from Ref. 27 (a) in the whole range, (b) in the UV-blue range, (c) and (d) around the $^5D_{0,1} \rightarrow {}^7F_J$ transitions.

at ~ 697 nm is observed, which is often present as impurity in Ga_2O_3.[48] It is unlikely that such emission originates from Cr^{3+} contaminants in sapphire, since the excitation depth of the electron beam is lower than 50 nm, well below the β-Ga_2O_3 thin film thickness.

The fact that a large fraction of Eu ions is in the 3+ valence state, is in accordance with CL and X-ray absorption near edge structure (XANES) results obtained for Eu-implanted/annealed β-Ga_2O_3 bulk single crystals.[27] The most intense emission is attributed to the $^5D_0 \rightarrow {}^7F_2$ transition located at ~ 611.5 nm, in agreement with previously reported values obtained for Eu-doped β-Ga_2O_3 nanostructures, fibers, thin films and bulk crystals.[22,23,26,27,49–51] The different $^5D_{0,1} \rightarrow {}^7F_J$ transitions represented in Fig. 4c, were assigned after a careful comparison with previous reports and presented in Table I in comparison with the measurements on Eu^{3+}-doped β-Ga_2O_3 nanocrystals from Ref. 23. For these transitions, the shape and the relative intensities of the Eu^{3+} intra-4*f* shell transitions are very similar for the Eu-implanted/annealed β-Ga_2O_3 thin films and bulk single crystals. However, below 590 nm in Fig. 4d, slight changes can be observed. Unlike β-Ga_2O_3 bulk single crystals[27] and β-Ga_2O_3 nanocrystals,[23] presenting one transition at 582 nm (at RT) or at 579.9 nm (at 10 K), the present thin films exhibit at least two transitions located at 579.7 and 582 nm, that can be attributed to $^5D_0 \rightarrow {}^7F_0$ and $^5D_0 \rightarrow {}^7F_0$ or $^5D_1 \rightarrow {}^7F_3$ transitions, respectively. Due to the singlet character of the $^7F_0$ fundamental and $^5D_0$ excited levels, the number of the observed $^5D_0 \rightarrow {}^7F_0$ transitions corresponds to the number of non-equivalent active sites in the Eu implanted sample.[17,52] Accordingly, at least one active site is created by the Eu-implantation/annealing in the β-Ga_2O_3 thin films, and the possibility of the presence of a second active site cannot be discarded. The Eu^{3+} ions in β-Ga_2O_3 can be incorporated in substitutional sites (Ga sites with octahedral and tetrahedral coordination) with Cs symmetry,[23] or it is possible that Eu is in a different crystalline environment caused by different (non-substitutional) sites or in substitutional sites with distortion induced by defects.[27] Furthermore, the transitions below 560 nm and better resolved in the present S2-Eu and S3-Eu thin films, in comparison to bulk single crystal, are suggested to be related to the $^5D_1 \rightarrow {}^7F_1$ and $^5D_1 \rightarrow {}^7F_2$ transitions. These assignments were obtained based on the transition energy calculations using the experimental values provided at 10 K by Zhu et al.,[23] as also included in Table I.

In Figs. 5a and 5b, combined excitation emission (CEE) spectra are represented for the S3-Eu sample in the UV and red regions, respectively. Due to the very low Eu^{3+} intra-4*f* shell transition intensity obtained for S1-Eu and S2-Eu samples, this part will be mainly dedicated to the β-Ga_2O_3 thin film with the highest thickness (S3-Eu sample), also showing the highest CL intensity of the $^5D_0 \rightarrow {}^7F_2$ transition. It is worth mentioning that unlike CL, PL measurements are scarce for Eu-implantated/annealed β-Ga_2O_3 material, and were only successfully achieved for nanowires, but not for bulk crystals. In our

Table I. Eu^{3+} ($4f^6$) intraionic transitions observed in the Eu implanted/annealed β-Ga_2O_3 thin films and corresponding assignments $^5D_{0,1}\rightarrow{}^7F_{0,1,2,3,4}$ in comparison with Zhu et al.[23]

Transitions (nm)	Present work CL at RT 10^{15} Eu ions.cm^{-2} implanted/annealed in MOVPE β-Ga_2O_3 thin films grown on sapphire	Zhu et al.[23] PL at 10 K Eu^{3+}-doped β-Ga_2O_3 NCs were synthesized by combustion
$^5D_1\rightarrow{}^7F_1$	534.8 540	533.2 538.3 541.4 532.3 537.4 540.4 531.6 536.7 539.7
$^5D_1\rightarrow{}^7F_2$	552	553.2 554.9 558.1 559.9 564.6 552.2 553.9 557.1 558.8 563.6 551.4 553.1 556.3 558.1 562.8
$^5D_0\rightarrow{}^7F_0$	579.7	579.9
$^5D_0\rightarrow{}^7F_0$ or $^5D_1\rightarrow{}^7F_3$	582	
$^5D_0\rightarrow{}^7F_1$	590 596	587.5 593.7 597.4
$^5D_0\rightarrow{}^7F_2$	611.7 617.7 621.4 626.6	611.8 613.9 617.8 620 625.8
$^5D_0\rightarrow{}^7F_3$	653.4 661.5	649 650.5 651.8 653 655.3 656.2 659.7
$^5D_0\rightarrow{}^7F_4$	707.4 712.6 717.8	682.1 692.9 698 703.9 704.7

case, CEE spectroscopy consists of measuring the emission spectrum for each excitation wavelength, from 250 to 265 nm, and from 250 to 300 nm, in the emission wavelength range close to the UV band (Fig. 5a), and the Eu^{3+} intra-4*f* shell transitions (Fig. 5b), respectively. The blue curves represent the PL spectra for S3-Eu sample, obtained under 260 nm (4.77 eV) excitation wavelength, resonant with the β-Ga_2O_3 bandgap value (obtained from transmission measurement). The PL response exhibits the UV band emission (Fig. 5a) and the Eu^{3+} and Cr^{3+} lines (Fig. 5b). The intensity ratio of Eu-related lines versus the UV band (∼1/10) is much lower than the one obtained by CL (∼5). It is reported that this ratio is strongly dependent on the excitation parameters, especially, on the excitation density.[23,26] Indeed, this is expected due to the low excitation density of the Xe lamp at 260 nm used in this measurement. Additional RT PL measurements on S3-Eu (not shown), using 160 nm excitation wavelength from a deuterium light source (lower excitation density than the Xe lamp), was only able to resolve the Cr^{3+} emission line, indicating that such excitation conditions are not promoting the Eu^{3+} intra-4*f* shell transitions. Fig. 5a and Fig. 5b demonstrate that efficient excitation of the UV band and the $^5D_0\rightarrow{}^7F_2$ most intense transition occurs through a broad excitation band around the bandgap energy of the β-Ga_2O_3 host (∼ 260 nm, 4.77 eV).

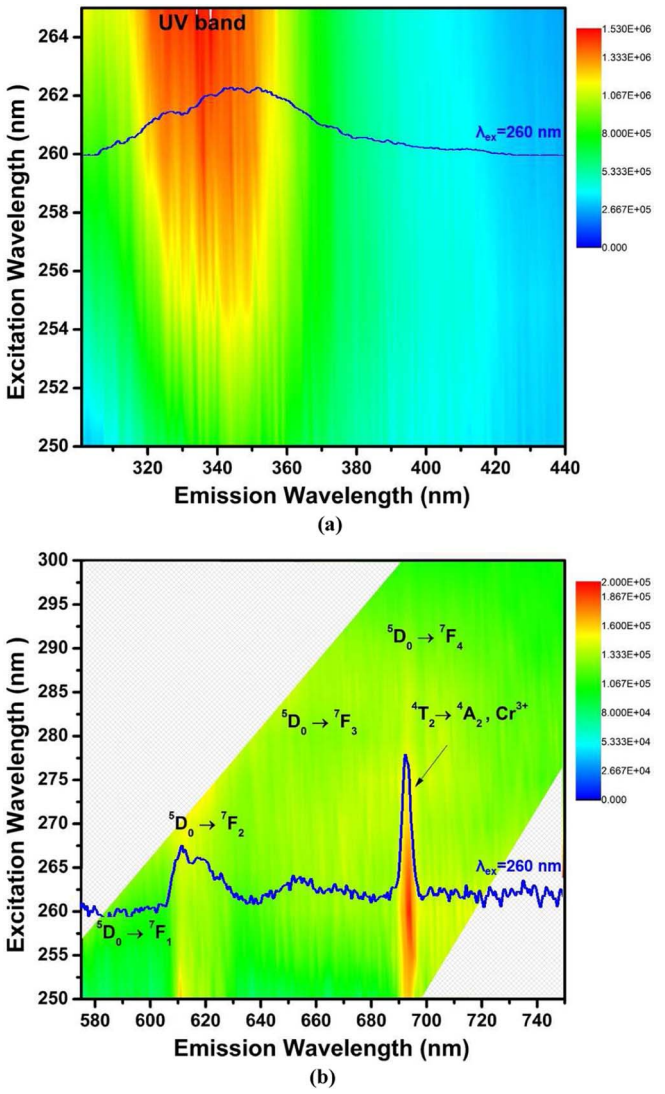

Figure 5. S3-Eu sample combined excitation emission (CEE) spectra represented in the UV (a) and red (b) regions. The blue curves represent the PL spectra for S3-Eu sample, obtained under 260 nm (4.77 eV) excitation in both regions.

Conclusions

In this work, we have established the effects of Eu implantation and annealing on β-Ga_2O_3 thin films grown by metal organic vapor phase epitaxy on sapphire substrate. The thin films were implanted with 300 keV Eu ions at 600°C, with a fluence of 1×10^{15} Eu·cm^{-2} and annealed at 900°C in flowing argon for 30 s. No significant changes neither additional peaks related to Eu complexes were detected in the XRD 2θ-ω scans, and no significant peak broadening or shifts are observed. RBS results and SRIM simulation are in good agreement, revealing that no Eu diffusion to the surface occurs. In the used implantation/annealing conditions, the Eu ion penetration depth reached ∼130 nm, with a maximum concentration at ∼50 nm. Furthermore, CL and PL/PLE results evidenced the optical activation of the Eu^{3+} in the β-Ga_2O_3 host. The detailed study of the Eu^{3+} intra-4*f* shell transitions revealed that at least one active site is created by the Eu implantation/annealing in β-Ga_2O_3 thin films grown on sapphire. The well controlled implantation and annealing process in β-Ga_2O_3 thin films pave the way for their use in optoelectronic applications, particularly in efficient red thin film electroluminescent devices.

Acknowledgments

The authors acknowledge financial support from FEDER funds through the COMPETE 2020 Programme and National funds through FCT - Portuguese Foundation for Science and Technology (FCT) under the projects UID/CTM/50025/2013, POCI-01-0145-FEDER-028011 & LISBOA-01-0145-FEDER-029666, and UID/FIS/50010/2019. B Mendez and E Nogales are grateful for the financial support from the MINECO (Projects No. MAT-2015-65274-R-FEDER and PCIN-2017-106). We especially thank Dr. Daniela Gogova for providing the as-grown samples of this study, for the availability and the fruitful discussions about β-Ga_2O_3 MOVPE growth.

ORCID

M. Peres https://orcid.org/0000-0001-6774-8492
K. Lorenz https://orcid.org/0000-0001-5546-6922
M. R. Correia https://orcid.org/0000-0003-3781-0085
T. Monteiro https://orcid.org/0000-0001-6945-2759
N. Ben Sedrine https://orcid.org/0000-0002-2255-3453

References

1. M. Higashiwaki and G. H. Jessen, "Guest Editorial: The dawn of gallium oxide microelectronics," *Appl. Phys. Lett.*, **112**, 060401 (2018), and references therein.
2. S. J. Pearton, Jiancheng Yang, Patrick H. Cary, F. Ren, Jihyun Kim, Marko J. Tadjer, and Michael A. Mastro, "A review of Ga_2O_3 materials, processing, and devices," *Appl. Phys. Rev.*, **5**, 011301 (2018).
3. E. G. Víllora, K. Shimamura, Y. Yoshikawa, K. Aoki, and N. Ichinose, "Large-size β-Ga_2O_3 single crystals and wafers," *Journal of Crystal Growth*, **270**(3–4), 420 (2004).
4. V. E. Chelnokov, A. L. Syrkin, and V. A. Dmitriev, "Overview of SiC power electronics," *Diamond and Related Materials*, **6**(10), 1480 (1997).
5. D. Gogova, P. P. Petrov, M. Buegler, M. R. Wagner, C. Nenstiel, G. Callsen, M. Schmidbauer, R. Kucharski, M. Zajac, R. Dwilinski, M. R. Phillips, A. Hoffmann, and R. Fornari, "Structural and optical investigation of non-polar (1-100) GaN grown by the ammonothermal method," *Journal of Applied Physics*, **113**(20), 203513 (2013).
6. M. Hermann, D. Gogova, D. Siche, M. Schmidbauer, B. Monemar, M. Stutzmann, and M. Eickhoff, "Nearly stress-free substrates for GaN homoepitaxy," *J. Cryst. Growth*, **293**(2), 462 (2006).
7. D. Gogova, H. Larsson, R. Yakimova, Z. Zolnai, I. Ivanov, and Bo Monemar, "Fast growth of high quality GaN," *Physica Status Solidi (a)*, **200**(1), 13 (2003).
8. M. Razeghi, Ji-H. Park, R. McClintock, D. Pavlidis, F. H. Teherani, D. J. Rogers, B. A. Magill, G. A. Khodaparast, Y. Xu, J. Wu, and V. P. Dravid, "A Review of the Growth, Doping & Applications of β-Ga_2O_3 thin films," *Proc. of SPIE*, **10533**, 105330R (2018).
9. A. Pérez-Tomás, E. Chikoidze, M. R. Jennings, S. A. O. Russell, F. H. Teherani, P. Bove, E. V. Sandana, and D. J. Rogers, "Wide and ultra-wide bandgap oxides: where paradigm-shift photovoltaics meets transparent power electronics," *Proc. of SPIE.* **10533**, 105331Q (2018).
10. E. Chikoidze, D. J. Rogers, F. H. Teherani, C. Rubio, G. Sauthier, H. J. Von Bardeleben, T. Tchelidze, C. Ton-That, A. Fellous, P. Bove, E. V. Sandana, Y. Dumont, and A. Perez-Tomas, "Puzzling robust 2D metallic conductivity in undoped β-Ga_2O_3 thin films," *Materials Today Physics*, **8**, 10 (2019).
11. T. Miyata, T. Nakatani, and T. Minami, "Gallium oxide as host material for multicolor emitting phosphors", *J. Lumin.*, **87–89**, 1183 (2000).
12. P. Gollakota, A. Dhawan, P. Wellenius, L. M. Lunardi, and J. F. Muth, "Optical characterization of Eu-doped β-Ga_2O_3 thin films," *Appl. Phys. Lett.*, **88**, 221906 (2006).
13. T. Monteiro, C. Boemare, M. J. Soares, R. A. Sa Ferreira, L. D. Carlos, K. Lorenz, R. Vianden, and E. Alves, "Photoluminescence and Lattice Location of Eu and Pr Implanted GaN Samples." *Phys. B*, **308**−**310**, 22 (2001).
14. K. O'Donnell and V. Dierolf, *Rare Earth Doped III-Nitrides for Optoelectronic and Spintronic Applications*, Canopus Academic Publishing Limited, Springer, 2010.
15. J. Rodrigues, M. F. Leitao, J. F. C. Carreira, N. Ben Sedrine, N. F. Santos, M. Felizardo, T. Auzelle, B. Daudin, E. Alves, A. J. Neves, M. R. Correia, F. M. Costa, K. Lorenz, and T. Monteiro, "Spectroscopic Analysis of Eu^{3+} Implanted and Annealed GaN Layers and Nanowires," *J. Phys. Chem. C*, **119**, 17954 (2015).
16. J. Rodrigues, M. F. Leitao, J. F. C. Carreira, N. Ben Sedrine, N. F. Santos, M. Felizardo, T. Auzelle, B. Daudin, E. Alves, A. J. Neves, M. R. Correia, F. M. Costa, K. Lorenz, and T. Monteiro, "Correction to "Spectroscopic Analysis of Eu^{3+} Implanted and Annealed GaN Layers and Nanowires"," *J. Phys. Chem. C*, **120**, 6907 (2016).
17. N. Ben Sedrine, J. Rodrigues, D. Nd. Faye, A. J. Neves, E. Alves, M. Bockowski, V. Hoffmann, M. Weyers, K. Lorenz, M. R. Correia, and T. Monteiro, "Eu-Doped AlGaN/GaN Superlattice-Based Diode Structure for Red Lighting: Excitation Mechanisms and Active Sites," *ACS Appl. Nano Mater.*, **1**, 3845−3858 (2018), and references therein.
18. N. Ben Sedrine, J. Rodrigues, J. Cardoso, D. Nd. Faye, M. Fialho, S. Magalhães, A. F. Martins, A. J. Neves, E. Alves, M. Bockowski, V. Hoffmann, M. Weyers, K. Lorenz, M. R. Correia, and T. Monteiro, "Optical investigations of europium ion

implanted in nitride-based diode structures," *Surface & Coatings Technology*, **355**, 40 (2018).
19. Rare Earth and Transition Metal Doping of Semiconductor Materials: Synthesis, Magnetic Properties and Room Temperature Spintronics; V. Dierolf, I. T. Ferguson, and J. M. Zavada, Eds.; *Woodhead Publishing Series in Electronic and Optical Material 87*, Elsevier, 2016.
20. J. Cardoso, N. Ben Sedrine, A. Alves, M. A. Martins, M. Belloeil, B. Daudin, D. Nd. Faye, E. Alves, K. Lorenz, A. J. Neves, M. R. Correia, and T. Monteiro, "Multiple optical centers in Eu-implanted AlN nanowires for solid-state lighting Applications," *Appl. Phys. Lett.*, **113**, 201905 (2018).
21. P. Wellenius, A. Suresh, and J. F. Muth, "Bright, low voltage europium doped gallium oxide thin film electroluminescent devices," *Appl. Phys. Lett.*, **92**, 021111 (2008).
22. N. F. Santos, J. Rodrigues, A. J. S. Fernandes, L. C. Alves, E. Alves, F. M. Costa, and T. Monteiro, "Optical properties of LFZ grown β -Ga_2O_3:Eu^{3+} fibres," *Applied Surface Science*, **258**(23), 9157 (2012).
23. H. Zhu, R. Li, W. Luo, and X. Chen, "Eu^{3+}-doped β-Ga_2O_3 nanophosphors: annealing effect, electronic structure and optical spectroscopy," *Phys. Chem. Chem. Phys.*, **13**, 4411 (2011).
24. P. Marwoto, S. Sugianto, and E. Wibowo, "Growth of europium-doped gallium oxide (Ga_2O_3:Eu) thin films deposited by homemade DC magnetron sputtering," *Journal of Theoretical and Applied Physics*, **6**, 17 (2012).
25. Z. Chen, K. Saito, T. Tanaka, M. Nishio, M. Arita, and Q. Guo, "Low temperature growth of europium doped Ga_2O_3 luminescent films," *Journal of Crystal Growth*, **430**(15), 28 (2015).
26. K. Lorenz, M. Peres, M. Felizardo, J. G. Correia, L. C. Alves, E. Alves, I. López, E. Nogales, B. Méndez, J. Piqueras, M. B. Barbosa, J. P. Araújo, J. N. Gonçalves, J. Rodrigues, L. Rino, T. Monteiro, E. G. Villora, and K. Shimamura, Doping of Ga_2O_3 bulk crystals and NWs by ion implantation, *Proc. SPIE 8987*, Oxide-based Materials and Devices V, 89870M (2014).
27. M. Peres, K. Lorenz, E. Alves, E. Nogales, B. Méndez, X. Biquard, B. Daudin, E. G. Víllora, and K. Shimamura, "Doping β-Ga_2O_3 with europium: influence of the implantation and annealing temperature," *J. Phys. D: Appl. Phys.*, **50**, 325101 (2017).
28. D. Gogova, M. Schmidbauer, and A. Kwasniewski, "Homo- and heteroepitaxial growth of Sn-doped β-Ga_2O_3 layers by MOVPE," *CrystEngComm*, **17**, 6744 (2015).
29. S. I. Stepanov, V. I. Nikolaev, V. E. Bougrov, and A. E. Romanov, "Gallium Oxide: Properties and Applications - A review," *Rev. Adv. Mater. Sci.*, **44**, 63 (2016).
30. J. F. Ziegler and J. P. Biersack, *The Stopping and Range of Ions in Matter.*, In: D. A. Bromley (eds) Treatise on Heavy-Ion Science. Springer, Boston (1985).
31. N. P. Barradas, C. Jeynes, and R. P. Webb, "Simulated Annealing Analysis of Rutherford Backscattering Data," *Appl. Phys. Lett.*, **71**, 291 (1997).
32. N. P. Barradas, C. Jeynes, and M. A. Harry, "RBS/Simulated Annealing Analysis of Iron-Cobalt Silicides," *Nucl. Instrum. Methods B*, **136**, 1163 (1998).
33. N. P. Barradas, C. Jeynes, R. P. Webb, U. Kreissig, and R. Grötzschel, "Unambiguous automatic evaluation of multiple Ion Beam Analysis data with Simulated Annealing *Nucl*." *Instruments Methods Phys. Res. Sect. B Beam Interact. with Mater. Atoms*, **149**, 233 (1999).
34. E. Nogales, P. Hidalgo, K. Lorenz, B. Méndez, J. Piqueras, and E. Alves, "Cathodoluminescence of rare earth implanted Ga_2O_3 and GeO2 nanostructures" *Nanotechnology*, **22**, 285706 (2011).
35. Joint Committee on Powder Diffraction Standards (JCPDS, PDF no. 43043-1012 and 041-1103).
36. D. A. Zatsepin, D. W. Boukhvalov, A. F. Zatsepin, Y. A. Kuznetsova, D. Gogova, V. Ya. Shur, and A. A. Esin, "Atomic structure, electronic states, and optical properties of epitaxially grown β-Ga_2O_3 layers," *Superlattices Microstruct.*, **120**, 90 (2018).
37. D. Gogova, G. Wagner, M. Baldini, M. Schmidbauer, K. Irmscher, R. Schewski, Z. Galazka, M. Albrecht, and R. Fornari, "Structural properties of Si-doped β-Ga_2O_3 layers grown by MOVPE," *Journal of Crystal Growth*, **401**, 665 (2014).
38. K. Shimamura, E. G. Víllora, T. Ujiie, and K. Aoki, "Excitation and photoluminescence of pure and Si-doped β-Ga_2O_3 single crystals," *Appl. Phys. Lett.*, **92**, 201914 (2008).
39. T. Onuma, S. Fujioka, T. Yamaguchi, M. Higashiwaki, K. Sasaki, T. Masui, and T. Honda, "Correlation between blue luminescence intensity and resistivity in β-Ga_2O_3 single crystals," *Appl. Phys. Lett.*, **103**, 041910 (2013).
40. T. Harwig, G. J. Wubs, and G. J. Dirksen, "Electrical properties of β-Ga_2O_3 single crystals," *Solid State Commun.* **18**, 1223 (1976).
41. Y. J. Park, C. S. Oh, T. H. Yeom, and Y. M. Yu, "Ammonolysis of Ga_2O_3 and its application to the sublimation source for the growth of GaN film," *J. Cryst. Growth*, **264**, 1 (2004).
42. K. Nishihagi, Z. Chen, K. Saito, T. Tanaka, and Q. Guo, "Structural properties of Eu doped gallium oxide films," *Mater. Res. Bull.*, **94**, 170 (2017).
43. T. Harwig and F. Kellendonk, "Some observations on the photoluminescence of doped β-galliumsesquioxide" *J. Solid State Chem.*, **24**, 255 (1978).
44. L. Binet and D. Gourier, "Origin of the blue luminescence of β-Ga_2O_3" *J. Phys. Chem. Solids*, **59**, 1241 (1998).
45. J. Zhang, B. Li, C. Xia, G. Pei, Q. Deng, Z. Yang, W. Xu, H. Shi, F. Wu, Y. Wu, and J. Xu, "Growth and spectral characterization of β-Ga_2O_3 single crystals" *J. Phys. Chem. Solids*, **67**, 2448 (2006).
46. A. Y. Polyakov, N. B. Smirnov, I. V. Shchemerov, E. B Yakimov, S. J. Pearton, Fan Ren, A. V. Chernykh, D. Gogova, and A. I. Kochkova, "Electrical Properties, Deep Trap and Luminescence Spectra in Semi-Insulating, Czochralski β-Ga_2O_3 (Mg)," *ECS Journal of Solid State Science and Technology*, **8**(7), Q3019 (2019).
47. E. Alves, C. Marques, N. Franco, L. C. Alves, M. Peres, M. J. Soares, and T. Monteiro, "Damage recovery and optical activity in europium implanted wide gap oxides," *Nucl. Instruments Methods Phys. Res. Sect. B Beam Interact. with Mater. Atoms*, **268**, 3137 (2010).
48. Y. Tokida and S. Adachi, "Photoluminescent Properties of Eu^{3+} in Ga_2O_3:Cr3+ Films Prepared by Metal Organic Deposition," *Jap. J. Appl. Phys.*, **52**, 101102 (2013).
49. E. Nogales, B. Méndez, J. Piqueras, and J. A. García, "Europium doped gallium oxide nanostructures for room temperature luminescent photonic devices," *Nanotechnology*, **20**, 115201 (2009).
50. P. Wellenius, E. R. Smith, S. M. LeBoeuf, H. O. Everitt, and J. F. Muth, "Optimal composition of europium gallium oxide thin films for device applications," *J. Appl. Phys.*, **107**, 103111 (2010).
51. I. Lopez, K. Lorenz, E. Nogales, B. Mendez, J. Piqueras, E. Alves, and J. A. Garcia, "Study of the relationship between crystal structure and luminescence in rare-earth-implanted Ga_2O_3 nanowires during annealing treatments," *J. Mater. Sci.*, **49**, 1279 (2014).
52. H. Peng, C. W. Lee, H. O. Everitt, C. Munasinghe, D. S. Lee, and A. J. Steckl, "Spectroscopic and Energy Transfer Studies of Eu^{3+} Centers in GaN." *J. Appl. Phys.*, **102**, 073520 (2007) and references therein.